Journal of Wind Engineering & Industrial Aerodynamics 168 (2017) 81–90

Contents lists available at ScienceDirect

Journal of Wind Engineering & Industrial Aerodynamics

journal homepage: www.elsevier.com/locate/jweia

Aerodynamic flow control for a generic truck cabin using synthetic jets

G. Minelli [a, *], E. Adi Hartono [a], V. Chernoray [a], L. Hjelm [b], S. Krajnović [a]

[a] Department of Applied Mechanics, Chalmers University of Technology, Gothenburg, Sweden
[b] Volvo Trucks AB, Gothenburg, Sweden

ARTICLE INFO

Keywords:
AFC
Drag reduction
Synthetic jet
Truck
Vehicle aerodynamic
Experiments

ABSTRACT

This experimental work presents the achievement in drag reduction with the use of active flow control (AFC) for a generic bluff body. Experiments were done in the Chalmers University closed loop wind-tunnel at Reynolds number $Re = 5 \times 10^5$. The Re is based on the undisturbed velocity $U_{inf} = 20$ m/s and the width of the model $W = 0.4$ m. The model consists of a simplified truck cabin, characterized by sharp edge separation on top and bottom edges and pressure induced separation on the rounded vertical side edges. The pressure induced separation reproduces the flow detachment occurring at the front A-pillar of a real truck. The investigation of the unactuated and actuated flow was conducted by means of time-resolved particle image velocimetry (PIV). Loudspeakers were used as the actuation device. These were characterized before the actuation study, highlighting an interesting analogy between actuation frequency and jet vortex pair size. The effects of different actuations were evaluated with hot wire anemometry. The effect of the actuation was studied using phase averaging and modal analysis. A notable reduction of the side recirculation bubble was observed. The nature of the separation mechanism was investigated and related to different actuation frequencies spanning the range $1 < F^+ < 6.2$. As for the Re, the non-dimensional frequency F^+ is based on the undisturbed velocity U_{inf} and the width of the model W.

1. Introduction

The past two decades have experienced the exponential growth of an actuation technology known as “synthetic jet”. The main feature of a synthetic jet lies in the capacity to generate a jet flow using the working fluid of the flow system. In this way, no complex piping is necessary to recreate a sinusoidal jet signal able to manipulate the surrounding flow field. This technique turned out to be versatile for different flow control applications. Aeronautic researchers were the principle investigators of this technique. The study pursued in order to enhance the aerodynamic performance of a post-stall aerofoil pushed the investigators to find a non-invasive technique that satisfies the following requirements:

- It should be easily adaptable to the flow conditions.
- It should introduce momentum in the boundary layer upstream of separation.
- It should be embedded in the surface of the aerofoil.
- It should use a limited level of energy.

A synthetic jet is able to meet all these requirements. The mechanical motion of a solid membrane opens the possibility to easily modulate the amplitude and frequency of a sinusoidal jet flow. The first attempts to control the flow separation by means of acoustic excitement of the boundary layer have been reported by different authors (Huang et al., 1987; Hsiao et al., 1990, 1994). The investigators observed a post-stall increase in lift, that was later quantified up to 50% (Chang et al., 1992). The later published works (Seifert et al., 1996; Wu et al., 1998; Amitay and Glezer, 2002a, 2002b; Smith, 2002; Glezer et al., 2005) asserted its potential. Several reviews, collecting old and the latest achievements, were published during the years (Gad-el Hak et al., 1998; Amitay and Cannelle, 2006; Cattafesta and Sheplak, 2011; Brunton and Noack, 2015), although, the work proposed in Glezer (2011) identifies an interesting and essential distinction based on the control frequency. Here, the author distinguishes the presence of two synthetic jet control strategies. The first approach employs low frequencies, which interact with the global flow instability. In this way, the actuation is able to lock the separated flow motion to its own frequency. The second strategy employs higher frequencies, out of the range of the so-called “receptive band”. In this case, as mentioned by the author, the control frequency is decoupled from the global instability of the base flow. The remarkable results that are cited have attracted various investigators and opened the possibility to adapt this control strategy to bluff bodies. Transport vehicles (e.g. trains, trucks, ships and cars) are indeed characterized by heavily separated flow. Always inspired by previous aeronautic

* Corresponding author.
E-mail address: minelli@chalmers.se (G. Minelli).

http://dx.doi.org/10.1016/j.jweia.2017.05.006
Received 3 February 2017; Received in revised form 19 April 2017; Accepted 20 May 2017

achievements, the aerodynamics of vehicles has significantly evolved, starting from the early 1980s, and this has enhanced their efficiency. The work of Choi (Choi et al., 2014), Ahmed (Ahmed et al., 1985), Modi (Modi et al., 1995) and Cooper (2003) are just a few examples of many achievements this research has produced over time. In the same way, the manipulation of the flow by an active flow control strategy can produce a drastic reduction of aerodynamic drag and, as a consequence, a significant reduction in fuel consumption as shown in Seifert et al. (2015); McNally et al. (2015). Several studies have pursued the reduction of bluff body separated flow regions and a reduction of the aerodynamic drag by means of different control strategies: from plasma actuators (Vernet et al., 2015) to pulsating jets (Krajnović et al., 2010; Barros et al., 2016) and synthetic jets (Ben Chiekh et al., 2013). The present work provides a novel study, to the knowledge of the authors, in its attempt to adopt the synthetic jet control strategy, used for aerofoil, to manipulate the flow separation occurring at the A-pillar of a truck cabin. This experimental work is part of an ongoing investigation of a control approach of the separated flow region in trucks. Earlier work in the same project can be found in Minelli et al. (2016). Looking closer at the flow features of a truck, there are four main sources of drag due to massive flow separation: the wheels and underbody, the wake, the gap between the tractor and trailer, and the front separation, Fig. 1a. This work focuses on the front separation occurring at the A-pillar of a truck cabin, Fig. 1b. A simplified model was chosen to reproduce the A-pillar flow separation and to control its behaviour, Fig. 2 and Table 1, achieving the following goals:

- A characterization of the actuation is reported, with the aim to investigate the formation of the jet vortex pair at different actuation frequencies.
- The flow of unactuated and actuated cases is investigated by means of time-resolved PIV.
- The unactuated flow snapshots are post processed by means of Proper Orthogonal Decomposition (POD) and Fast Fourier Transform (FFT) analyses.
- Four different actuation frequencies are chosen following the modal analysis and the achievements described in Minelli et al. (2016).
- The reduction of the side recirculation bubble is achieved and described for all actuations.
- The physics defining each actuated case is described (by means of a phase averaging of the PIV snapshots), corroborating the presence of a "receptive band" of frequencies (Glezer et al., 2005).
- The downstream effect of the actuation in the wake of the model is studied.

2. The experimental set-up

The model consists of a simplified truck cabin, characterized by sharp edge separation on top and bottom edges and pressure induced separation on the rounded vertical front edges. The pressure induced separation reproduces the flow detachment occurring at the front A-pillar of a real truck cabin. The model was designed to highlight the A-pillar separation, which was studied in detail. In particular, two of the domains observed (Fig. 3b) were investigated by means of time-resolved PIV. Fig. 2a and b shows the model during the assembly stage. Four speakers (WAVECOR SW182BD01) were employed to reproduce the jet flow described in Fig. 4b. Once the front and the top lid of the model were assembled, the speakers were sealed to avoid air leakages. Fig. 2c and Table 1 present the model and test section's main dimensions. All the dimensions are scaled by the model width, $W = 0.4$ m. The model is defined by a square cross-section, where width and height have the same dimension.

Experiments were carried out in a closed circuit wind-tunnel at Chalmers University of Technology. The test section dimensions are $3.00 \times 1.80 \times 1.25$ m^3, and the speed range is 0–60 m/s. The flow turbulence level was within 0.15%. Fig. 2c shows the model placed in the wind-tunnel test section. Hot wire measurements were made to characterize the jet flow at the actuation slot. The velocity traces were phase-averaged over 500 blowing and suction cycles. Since the hot wire measurement technique is not able to distinguish the flow direction, a correction was implemented for the suction part of the cycle. Thus, it was initially inverted to reflect the correct behaviour of the flow. During this operation, the wind tunnel was turned off to record only the jet flow at the slot. In this way, and knowing the actuation frequency, it was easier to distinguish the flow direction, i.e. the blowing or suction part of the cycle. PIV images were registered by a monochrome double-frame SCMOS camera SpeedSense M340 by Dantec with a 2560-pixel by 1600-pixel resolution, 12-bit pixel depth, and 10-μm pixel size. The camera was equipped with a 105-mm f/2.8 lens from Sigma. The camera registered image pairs at a 400 Hz frame rate at full resolution in double frame mode. Flow seeding was achieved with a fog generator and a glycol based fluid. The Dual Power Nd:YLF LDY300-PIV laser from Litron provided up to 2×30 mJ at 1000 Hz and a 527-nm wavelength. The laser was equipped with a laser guiding arm and laser sheet optics. The flow field area illuminated was 200×400 mm^2. Dantec Dynamic Studio 2015 software was used for data acquisition and post-processing. Each data set included 800 images, which corresponds to a measurement period of 2 s with a spatial resolution of 0.125×0.156 mm^2 per pixel. The vector calculation was performed in a multi-pass procedure with a decreasing window size. The initial interrogation window size was 64-pixel $\times$ 64-pixel with a 50% overlap and square 1:1 weighing factor for the first two passes. Finally, three passes were performed with a 32-pixel $\times$ 32-pixel window size, 50% overlap and a round 1:1 Gaussian weighing factor. 2D snapshots of the flow were recorded during the experiments. Velocity components were recorded in two planar regions at $z = H/2$, Fig. 3. The snapshots captured were used for POD and FFT analyses and phase averaging. Fig. 3 shows the dimensions of the observed domains.

2.1. Modal and frequency analyses

One single POD temporal coefficient can oscillate at different frequencies, while the FFT analysis highlights the area of interest of the actual frequencies of the flow. It is interesting to compare the two approaches in order to gain a complete understanding of the flow structures in terms of both the energy content and characteristic frequencies.

The POD here is made on velocity snapshots sampled with a constant time step. For example the wall normal velocity component set of snapshots is described by $v^m = v(\mathbf{x}, t^m)$ at time $t^m = m\Delta t$, $m = 1, \ldots, M$ with the time Δt, and a Cartesian coordinate system $\mathbf{x} = (x, y, z)$ with unit vectors $\mathbf{e}_x$, $\mathbf{e}_y$, $\mathbf{e}_z$ respectively.

As was originally proposed by Lumley (1970), this method is based on

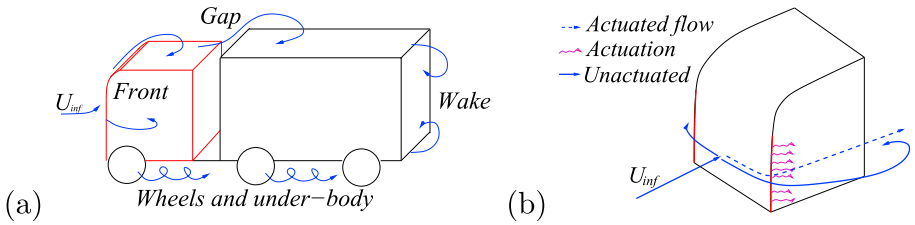

Fig. 1. Main sources of aerodynamic drag for a truck (a). The A-pillar separation and the effect of the actuation (b).